Nanoscale

Accepted Manuscript

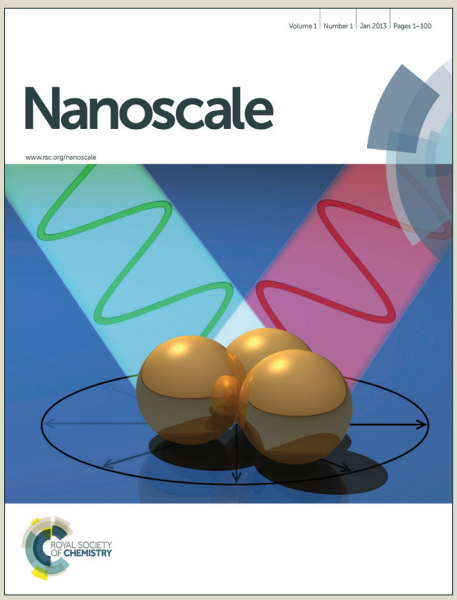

ROYAL SOCIETY OF CHEMISTRY

www.rsc.org/nanoscale

Ordered mesoporous Ag superstructure synthesized via template strategy for surface-enhanced Raman spectroscopy

Cuifeng Tian[†, ‡], Jiang Li[†], Chunsheng Ma[†], Ping Wang[‡], Xiaohong Sun[§,*], Jixiang Fang[†,*]

[†] *School of Science, Key Laboratory of the Ministry of Education and International Center for Dielectric Research, Xi'an Jiaotong University, Shann xi, 710049, China*

[‡] *School of Physics and Electronic Science, Shanxi Datong University, Shanxi 037009, P. R. China*

[§] *School of Materials Science and Engineering, TianJin University, Tianjin, 300072, China*

ABSTRACT

The surface-enhanced Raman scattering (SERS) substrates with high density and uniformity of nanogaps are proofed to enhance the reprodiciblity and sensitivity of Raman signal. Up to now, the syntheses of highly ordered gold or silver superstructure with controllable nanoparticle size and well-defined particle gap are still quite limited. Here, we reported an ordered mesoporous silver superstructure replicated by using ordered mesoporous KIT-6 and SAB-15 as templates. By means of a nanocasting process, the ordered mesoporous Ag superstructure was successfully synthesized, which shows uniform distribution of nanowire diameter (10 nm) and nanogap size (~2 nm), thus exhibits high Raman enhancement of ~10^9. The finite difference time-domain (FDTD) results indicate that ordered mesoporous Ag superstructure have a uniform distribution of hot spots. Therefore, the mesoporous silica template strategy presented here could lead to a new class of high quality SERS substrate and open extraordinary potentials for diverse applications.

KEYWORDS: orderly porous template, superstructure, SERS, FDTD

Surface-enhanced Raman spectroscopy (SERS) is characterized by a rather large amplification of the weak spontaneous Raman signal. The origin of this enhancement is shown to rely on the surface plasmon resonance (SPR) between the laser and metal nanostructure.[1, 2] It is known that the surface plasmonic couplings usually occur at SERS-active sites, including several nanometer gap junctions (defined 'hot spots') or tips around which induces giant electromagnetic enhancement.[3-5] However, the random distribution of hot spots results in a wide distribution of EF values and obtains irreproducible SERS signals.[6] In addition, the relatively low density of SERS-active sites obtained via lithographic route make SERS signal poor uniform, particularly at ultralow molecule concentrations, because, in this case, quite a few dye molecules might not land inside hot spots although they could be precisely prefabricated.[7] Therefore, the center problem now is the well-definition of the hot spots, including how to reproducibly synthesize sub-5 nm nanogaps between nanopartciles, how to increase the density of the hot spots and how to regulate the uniformity of nanogap distance within SERS substrate.

At present, some outstanding approaches are available for controlling the nanogap size and density,[8-15] such as the self-assembly method,[8, 9] lithographic techniques,[10] the template strategy including AAO,[11] polymer template,[12] and 3D SiO_2 spheres template.[13] Although these substrates have made a great improvement in the control of gap size, there are fewer that are capable of meeting the requirements of a SERS-active substrate, for instance, small nanogaps and high hot spot density. Recently, Fang's group has successfully synthesized highly ordered mesoporous silver supercrystals (OMASC-28) by using an orderly porous template with large pore size up to 28 nm, which exhibited high SERS sensitivity.[15] Wang et al. has also obtained ordered polyhedral mesoporous Pt nanoparticles using the mesoporous template of KIT-6.[14] In fact, the obtained nanostructures can be well tailored to enhance the local field effect through selecting various

templates. For example, the hot spot density can be further increased by means of a template with small pore sizes, i.e less than ~10 nm. Moreover, using various templates, diverse mesostructures with controlled gap sizes and high hot spot density may be achieved (Figure 1a).

Herein we used two kinds of orderly mesoporous templates, e.g. the mesoporous silica KIT-6 and SBA-15 structures to prepare the highly ordered mesoporous Ag superstructure (OMAS) through dip-calcination method (described in experimental section). As a result, two typical mesostructures of the OMAS were obtained, including interconnected mesh structure and nanowire bundles as showed in Figure 1a. The nanoparticle diameter and gap size of Ag superstructure can be well controlled by the KIT-6 and SBA-15 templates (Figure 1a). Owing to the uniform and high density of nanogaps between nanoparticle building blocks, the OMAS can be promising to employ as high-quality SERS substrates. The plasmon enhancement performance was evaluated via the measurements of Raman spectroscopy and the electromagnetic field calculation using the finite difference time domain (FDTD) method. We found that the OMAS with appropriate nanowire diameter, i.e 10 nm, and the gap size of ~2 nm, displayed a highly effective SERS activity with high signal amplification reaching to ~10^9.

RESULT AND DISCUSSION

In this work, we chose ordered mesoporous silica KIT-6 and SBA-15 structures as templates to prepare the ordered mesoporous Ag superstructure (here, the diameter of nanoparticle is about 10 nm, so denoted OMAS-10). The KIT-6 template was synthesized according to the procedure in Ref [16]. The transmission electron microscopy (TEM) image of the ordered mesoporous silica template KIT-6 indicates that the template has a highly ordered structure with preferable arrangement along the [311] direction (Figure 1b) and [531] direction (Figure S1a) as described in previous report, [16] which displays cubic *Ia*3*d* symmetry. The pore size (about 8-10 nm) was estimated by the TEM

image (Figure 1b) and the small-angle X-ray scattering (SAXS) curve (Figure S1b). In Figure 1c, it is showed another ordered mesoporous template, i.e. SBA-15, by which nanowire morphology normally can be fabricated.[17]

The morphologies and structures of the obtained OMAS-10 by using calcinations method (as described in experimental section) after the remove of the hard template of SBA-15 and KIT-6 were showed in Figure 2 and Figure 3. From the lower magnification SEM image of OMAS-10 for nanowire bundles (Figure 2a), we can see that the size of nanowire bundles is about several micrometers and there are some discrete nanowires covered on the bundles. In the Figure 2b, it can be seen that the nanowires paralleled to each other and the diameter is about 9-10 nm, which is consistent with the pore size of parent template. By means of same processes of nanowire bundles, mesh morphology of OMAS-10 can also be obtained through calcinations (Figure 2c and Figure 2d). Similar morphologies show that the growth of silver nanoparticles was restricted within the parent template. Further, the comparison of the structure for the KIT-6 template and the OMAS-10 may further confirm this statement. In the Figure S1 and in Ref [16], the templates have different pore connecting ways which determine the morphologies of the OMAS-10 (shown in Figure S2). In the inset of Figure 2d, we can see one of the networks, which is replicated the {111} surface of the KIT-6 template.

The structural features of OMAS-10 are further elucidated from the TEM images as shown in Figure 3. From the Figure 3a and 3b, the individual nanowires distribute parallel to each other. The diameter of nanowire is about 10 nm and the gap between nanowires is around 2-3 nm. It is noted that some connecting nanoparticles can be observed between nanowires, which contribute to the structural stability of nanowire bundles even after removal of the silica template. For mesh morphology, the diameter of silver sphere is about 10 nm (as showed in the dotted circles of Figure

3d). The nanoparticles are connected by small necks with a distance between nanoparticle building blocks of around 2-5 nm (Figure 3d). The selective area electron diffraction (SAED) of the OMAS-10 is shown in Figure S3a, which confirms its polycrystalline nature. As one can see from the Figure S3b, the spacing of lattice planes is 0.23 nm for a single silver sphere, which is consistent with the space of (111) crystal plane of silver.[18] According to our previous processes, the silica template may be removed completely after washing by NaOH solution three times[15] and this can be confirmed by the energy dispersive X-ray spectrometry (EDS, in Figure S4), displaying no obvious oxygen element existing in the OMAS-10 specimens.

To gain deep insights into the properties of local surface plasmon resonance (LSPR) for the two mesostructures of OMAS-10, the finite difference time-domain (FDTD) calculation was carried out to understand the interaction between electromagnetic field and the OMAS-10 (the models are shown in Figure S5). From the comparison of electrical field intensity, one can see that the OMAS-10 with nanowire bundle structure displays a relatively higher enhancement capability than that of mesh structure at the excitation light wavelength of 514 nm and 633 nm (Figure 4a and 4c). Considering the uncertainty of the size of connecting rods, we studied the dependence of the connecting rod widths (w) on the electrical field amplification at the same silver sphere diameters (D=10 nm) and gap size (g=2 nm). The results showed that the field magnitude for the rod widths from 4-6 nm exhibits a comparable scale (Figure 4a and 4c), revealing that the width of connecting rod has little impact on the field enhancement of Ag superstructure when the diameter of silver and the gap size are given. Furthermore, one can see that the OMAS-10 for both two structures demonstrates the highest field enhancement with $|E|/|E_0|\sim 40$ at excitation wavelength of 785nm, which corresponds to a SERS enhacement (proportional to $\sim|E|^4$) of $\sim 10^6$. As for the calculated field enhancement factor, it is lower than the one obtained from the experiment (see below), which could

be attributed to the chemical contribution and the difference between the model and actual arrangements of OMAS-10.[19, 20] Figure 4b and Figure 4d are the calculated electromagnetic field distribution of the OMAS-10 at the 514 nm excitation wavelengths. Obviously, the maxima field enhancements are uniformly located in the gaps between Ag two spheres or two nanowires. In addition, owing to the small nanoparticle building blocks, i.e. ~10 nm for two structures, the FDTD results indicate that both the two models contribute to an ultrahigh hot spot density which can be also great benefit to the reprodiciblity for the SERS signal. Therefore, the OMAS-10 structure reported in this work could serve as an efficient SERS substrate to achieve a high sensitivity and repeatability of detected signal.

The SERS performance for two typical structures of the OMAS-10 was evaluated and showed in Figure 5. We examined the widely used dye molecules, crystal violet (CV) for SERS studies. To precisely determine the structure of OMAS-10 as well as its SERS activity requires electron and optical microscopic observations on the same region so as to ensure that the exact the same particle is characterized (Figure S6). Therefore, in this work, a silicon wafer patterned by electron beam lithography was employed as a substrate to support the synthesized OMAS-10 (Figure 5a). The Raman spectra for two kinds of OMAS-10 structures are shown in Figure 5b, which are measured at 514 nm excitation with the same CV concentrations, e.g. 10^{-7} M aqueous. The SERS spectra reveal the characteristic peaks of CV, for instance, at 1172, 1371, and 1619 cm^{-1}, and correspond well to the ordinary Raman spectra of CV in the solid state and in aqueous solution. One can see that the intensities of CV peak at ~1619 cm^{-1} are around 3200 and 6300 for mesh structure and nanowire bundles under the 514 nm excitation wavelength, respectively (Figure 5b). According to the procedure described in Ref [15, 21-26] for the CV molecules, the EFs of the OMAS-10 are estimated about 4.85×10^{8} for mesh structure and 1.03×10^{9} for nanowire bundle, respectively. This

result is consistent with that of theoretical calculation using the FDTD methods for two structures. To evaluate the limit of detection (LOD) for two kinds of structures of OMAS-10, a series of low concentrations of CV aqueous solution as SERS probe molecule ranging from 1 μM to 0.1 pM were measured. From Figure 5c and 5d, the nanowire bundle structure of OMAS-10 demonstrates a better sensitivity with a LOD down to 0.1 pM even less. While for the mesh structure of OMAS-10, the Raman spectrum seems can be identified at the level of 0.1 nM for CV molecules. Thus, the OMAS-10, particularly for nanowire bundle structures, can be exploited as high-quality SERS based sensing detection.

CONCLUSTION

In conclusion, we have successfully synthesized an ordered mesoporous Ag superstructure (OMAS-10) by the nanocasting process using mesoporous silica KIT-6 and SBA-15 as templates. The obtained structures with high density and uniform nanogaps (~1-3 nm) can be controlled by the parent template. Furthermore, such silver superstructure as a SERS substrate exhibits a high sensitivity on the magnitude of ~10^9 and the detection limit of the OMAS-10 with nanowire bundles can reach 0.1 pM levels for CV molecules. The FDTD calculation reveals that ordered silver superstructure have a uniform distribution of hot spots, which are particularly beneficial to the reprodiciblity for SERS. Therefore, we believe that the OMAS with controlled nanoparticle size and uniform gap will be an effective SERS substrate for organic chemical molecules, biomolecules, even at single molecule level.

EXPERIMENTAL SECTION

Chemicals. KIT-6 was supplied by Tianjin University (Tianjin, China). SBA-15 was purchased from Nanjing XFNANO Material Tech. Co., Ltd. Silver nitrate ($AgNO_3$) was purchased from Sigma. Hexamethyldisilazane (HMDS) was purchased from Sinopharm Chemical Reagent Co., Ltd. ethanol (C_2H_5OH) and sodium hydroxide (NaOH) were purchased from Tianjin Chemical corp.

Synthesis of OMAS-10 by dip-calcination method. In order to improve long-rang ordering in three dimensions according to the template direction, a modified dipping method was implemented. In this process, OMAS-10 was synthesized following methods reported elsewhere.[27] Briefly, the silica surface of KIT-6 or SBA-15 was modified with methyl groups by refluxing a mixture containing 0.039 g hexamethyldisilazane (HMDS), 30 mL of n-hexane and 0.2 g of calcined KIT-6 or SBA-15. The obtained material is denoted as HP-KIT-6 (hydrophobic KIT-6) or HP-SBA-15 (hydrophobic SBA-15). In order to synthesize the mesoporous silver, a solution containing 0.021 g of $AgNO_3$ (3M), was impregnated into 0.035 g of the HP-KIT-6 or HP-SBA-15through an incipient wetness method. After drying at 313 K for two days, the sample was heated to 573 K under nitrogen flow for 2 h. Then the silica template was completely removed by treating the composite material with 3 M NaOH solution three times at 310 K. Finally, the product of the mesoporous silver was washed with acetone and distilled water several times and dried at room temperature.

Characterization. The morphology and structure of mesoporous templates and OMAS-10 was observed using a scanning electron microscopy (SEM, JSM-7000F) and a transmission electron microscopic (TEM, JEM 2100). The small-angle X-ray scattering (SAXS) data were taken on a Bruker D8 Advance X-ray diffractometer with Cu Kα radiation (λ= 1.5406 Å). A scan rate of 0.018° min^{-1} was used to record the patterns in a 2θ range of 0.7°–3.0°.For measuring large area of OMAS-10 at the 10^{-7} M concentration of CV (as showed in Figure 4a), the Raman spectra was

measured with a confocal Raman microscope (LabRAM HR800) at the excitation wavelength of 514 nm from an argon ion laser, and the laser power was ~0.022 mW. The laser spot on a sample was ~0.8 μm in diameter under confocal mode. Raman signals were collected through the 100x objective in the backscattering geometry. The acquisition time was 2 s. For measuring the detection limit of OMAS-10, the Raman spectra were obtained by using Renishaw inVia Raman microscope at room temperature through 50X objective of a Leica microscope (1 mm laser spots). The wavelength of excitation laser is 514 nm and the power is 20 mW at the sample for less than 10 nmol, 2 mW for other concentration. The exposure time was 3 s.

Supporting Information Available. TEM images of KIT-6 template, SEM images of OMAS-10, details of FDTD simulation, optical parameters, and the estimation of SERS enhancement factor were included.

Corresponding Author

*E-mail: *jxfang@mail.xjtu.edu.cn*, *sunxh@tju.edu.cn*

Acknowledgements

This work was supported by National Natural Science Foundation of China (Nos.11304188 and 51171139), Doctoral Fund for New Teachers (Nos. 20130201110032 and 20110201120039), Fundamental Research Funds for the Central Universities (No xkjc2014004) and Scientific New Star Program in Shaanxi Province (No.2012KJXX-03).

REFERENCES

(1) Nie, S.; Emory, S. R. *Science* 1997, *275*, 1102-1106.

(2) Kneipp, K.; Wang, Y.; Kneipp, H.; Perelman, L.T.; Itzkan, I.; Dasari, R. R.; Feld, M. S. *Phys. Rev. Lett.* 1997, *78*, 1667-1670.

(3) Lim, D. K.; Jeon, K. S.; Hwang, J. H.; Kim, H.; Kwon, S.; Suh, Y. D.; Nam, J.M. *Nature Nanotech*. 2011, *6*, 452-460.

(4) Xu, H. X.; Bjerneld, E. J.; Käll, M.; Börjesson, L. *Phys. Rev. Lett.* 1999, *83*, 4357-4360.

(5) Xu, H. X.; Aizpurua, J.; Käll, M.; Apell, P. *Phys. Rev. E* 2000, *62*, 4318-4324.

(6) Li, W. Y.; Camargo, P. H. C.; Lu, X. M.; Xia Y. N. *Nano lett.* 2009, *9*, 485-490.

(7) Fang, Y.; Seong, N. H.; Dlott, D. D. *Science* 2008, *321*, 388-392.

(8) Thai, T.; Zheng, Y.; Ng, S. H.; Mudie, S. *Angew. Chem. Int. Ed*. 2012, *51*, 8732 –8735.

(9) Chen, A. Q.; Deprince III, A. E.; Demortiere, A.; Joshi-Imre, A.; Shevchenko, E. V.; Gray, S. K.; Welp, U.; Vlasko-Vlasov, V. K. *Small* 2011, *7*, 2365-2371.

(10) Im, H.; Bantz, K. C.; Lindquist, N. C.; Haynes, C. L.; Oh, S. H. *Nano Lett.* 2010, *10*, 2231–2236.

(11) Liu, X.; Shao, Y.; Tang, Y.; Yao, K. F. *Scientific Reports* 2014, *4*, 5835.

(12) Wu, Y. P.; Fei, Z.; Yang, L. B.; Liu, J. H. *Chem. Commun.* 2013, *49*, 5025-5027.

(13) Kuroda, Y.; Kuroda, K. *Angew. Chem. Int. Ed.* 2010, *49*, 6993 –6997.

(14) Wang, H. J.; Jeong, H. Y.; Imura, M.; Wang, L.; Radhakrishnan, L.; Fujita, N.; Castle, T.; Terasaki, O.; Yamauchi, Y. *J. Am. Chem. Soc.* 2011, *133*, 14526 -14529.

(15) Tian, C. F.; Deng, Y. H.; Zhao, D. Y.; Fang, J. X. *Adv. Optical Mater.* **2015,** *3*, 404-411.

(16) Kleitz, F.; Choi, S. H.; Ryoo, R. *Chem. Commun*. 2003, 2136-2137.

(17) Huang, M. H.; Choudrey, A.; Yang, P. D. *Chem. Commun.*, 2000, 1063–1064.

(18) Ding, C. H.; Tian, C. F.; Krupke, R.; Fang, J. X. *CrystEngComm*, 2012, *14*, 875-881.

(19) Doering, W. E.; Nie, S. M. *J. Phys. Chem. B* 2002, *106,* 311-317.

(20) Otto, A. The 'Chemical' (Electronic) Contribution to Surface-Enhanced Raman Scattering. *J. Raman Spectrosc.* 2005, *36*, 497-509.

(21) Wang, Y; Becker, M.; Wang, L.; Liu, J. Q.; Scholz, R.; Peng, J.; Gösele, U.; Christainsen, S. H.; Kim, D. H.; Steinhart, M. *Nano Lett.* 2009, *9*, 2384-2389.

(22) Cai, W. B.; Ren, B.; Li, X. Q.; She, C. X.; Liu, F. M., Cai, X.W.; Tian, Z. Q. *Surf. Sci.* 1998, *406*, 9-22.

(23) Fang, J. X.; Du, S. Y.; Lebedkin, S.; Li, Z. Y.; Kruk, R.; Kappes, M.; Hahn, H. *Nano Lett.* 2010, *10*, 5006-5013.

(24) Fang, J. X.; Liu, S. Y; Li, Z. Y. *Biomaterials.* 2011, *32*, 4877-4884.

(25) Tian, C. F.; Ding, C. H.; Liu, S. Y.; Yang, S. C.; Song, X. P.; Ding, B. J.; Li, Z. Y.; Fang, J. X. *ACS Nano.* 2011, *5*, 9442-9449.

(26) Liu, Z.; Yang, Z.; Peng, B.; Cao, C.; Zhang, C.; You, H.; Xiong, Q.; Li, Z. Y.; Fang, J. X. *Adv. Mater.* 2014, *26*, 2431-2439.

(27) Shon, J. K.; Kong, S. S.; Kim, J. M.; Ko, C. H.; Jin, M.; Lee, Y. Y.; Hwang, S. H.; Yoon,J. A.; Kim, J. N. *Chem. Commun.*, 2009, 650-652.

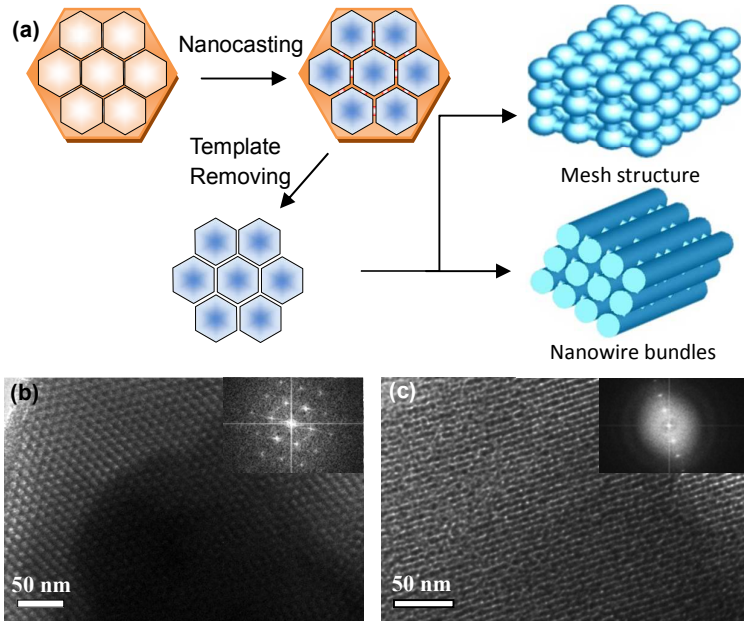

Figure 1 (a) Schematic diagram of the synthesis procedure for ordered silver superstructure by means of a nanocasting process using KIT-6 and SBA-15 templates. The low-magnification TEM image of ordered mesoporous silica template: (b) KIT-6; (c) SBA-15; inset (b) and (c) are the corresponding FFT diffractogram.

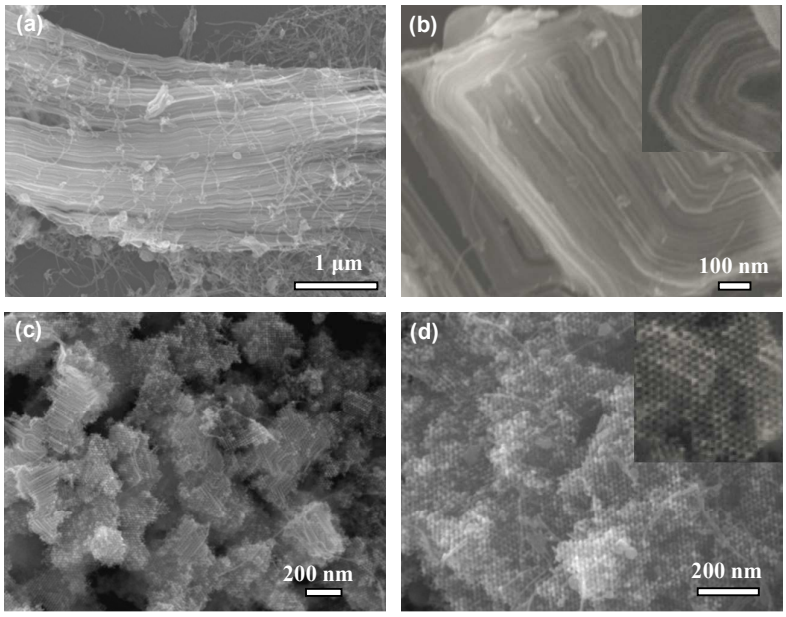

Figure 2 Low and high magnification SEM images of ordered mesoporous silver structures: (a)-(b) nanowire bundles obtained from the SBA-15 template; (c)-(d) mesh structure obtained from KIT-6 template.

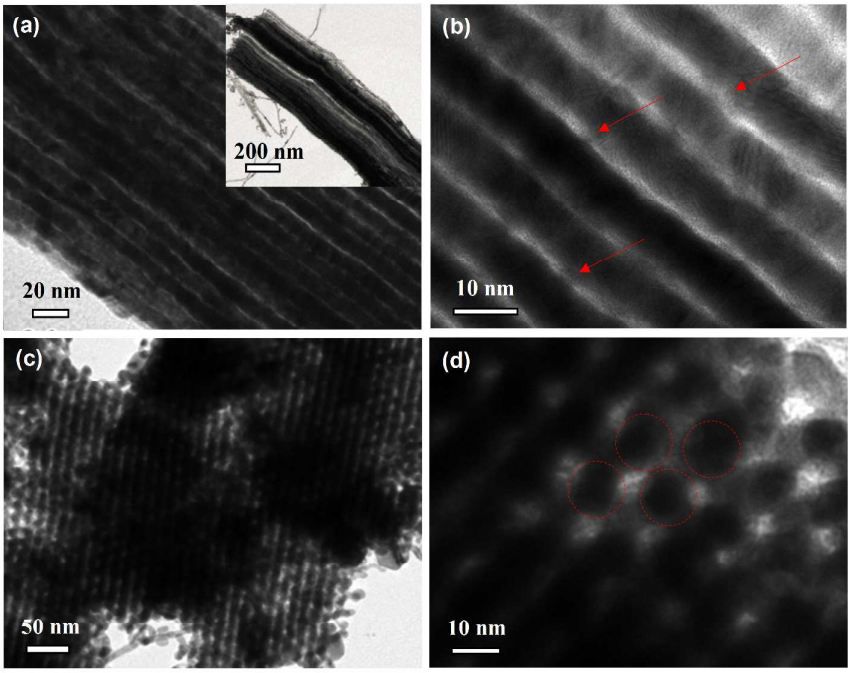

Figure 3 TEM images of the as-made highly mesoporous silver structure (OMAS-10) after removing the template: (a) - (b) nanowire bundles, (c) - (d) mesh structure.

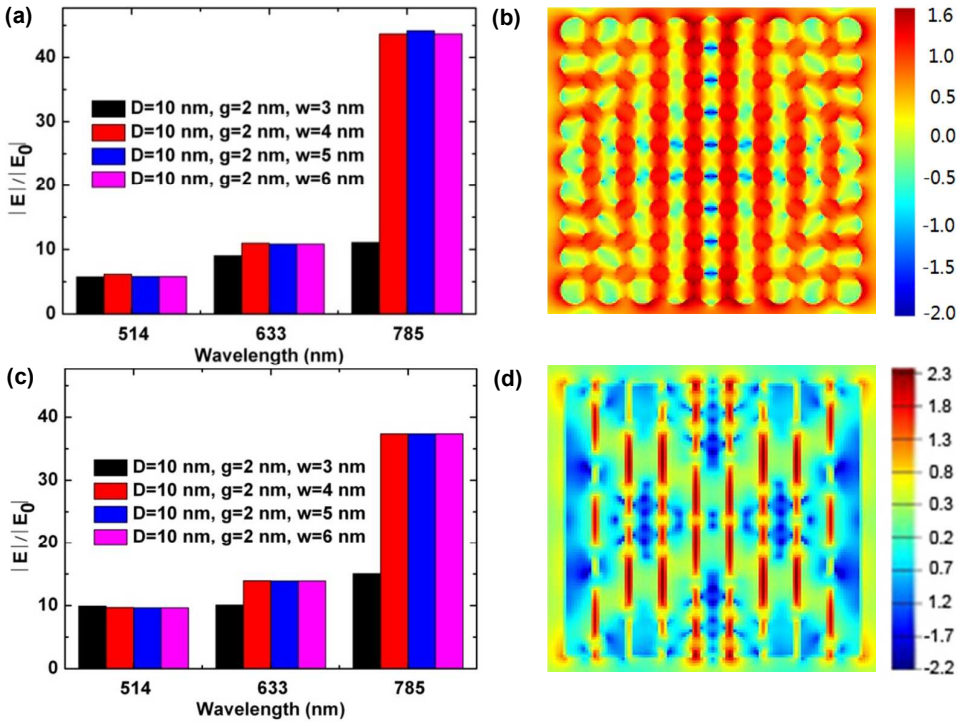

Figure 4 The histograms of field enhancements of two kinds of OMAS-10 as the functions of widths of connecting rod varied from 3 to 6 nm for three excitation wavelengths: (a) mesh structure. (c) nanowire bundles. (b) and (d) are the calculated E-field distributions and their E-field intensity of OMAS-10, D=10 nm, g=2 nm, w=5 nm for mesh and nanowire structure, respectively. The scale bars of electromagnetic field intensity $|E|^2$ have been plotted on a log-scale.

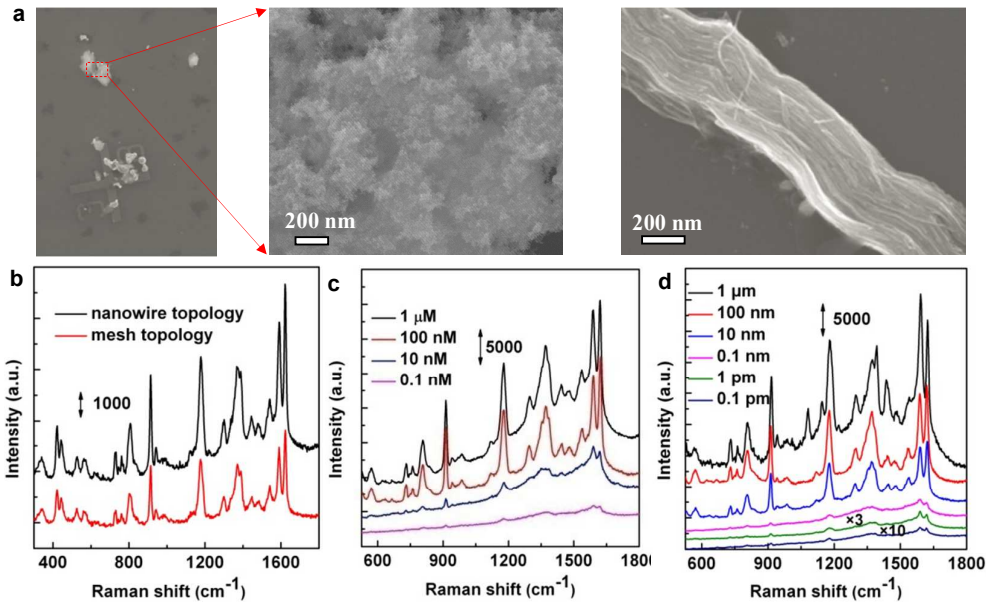

Figure 5 SEM image of the OMAS-10 on the marked silicon wafer: (a) mesh structure and nanowire bundles. SERS spectra of CV adsorbed on the OMAS-10 substrates, (b) the spectra of 10^{-7}M CV measured with a confocal Raman microscope (LabRAM HR800): a 514 nm excitation laser, 2 s acquisition times, 0.022 mw laser power and 100x objective lens. (c)–(d) SERS spectra of the OMAS for two structures, measured with Renishaw inVia Raman microscope (20 mw for less than 10 nmol and 2 mw for other concentration, 3 s acquisition times, and 50 x object lens) at different CV concentrations: (c) mesh structure; (d) nanowire bundles.